Diffusion in a Sol−Gel-Derived Medium with a View toward Biosensor Applications

Graham Hungerford,* Ana Rei, and M. Isabel C. Ferreira

Departamento de Física, Universidade do Minho, 4710-057 Braga, Portugal

Klaus Suhling and Carolyn Tregidgo

Department of Physics, Kings College London, Strand, London WC2R 2LS, United Kingdom

Received: September 15, 2006; In Final Form: December 20, 2006

Time-resolved fluorescence anisotropy and fluorescence recovery after photobleaching were applied to study the diffusion of dyes and a fluorescence-labeled enzyme in a sol−gel-derived medium. This type of medium exhibits attractive properties such as robustness, low processing temperature, high porosity, large internal surface area, and can act as protective immobilization media for biologically active molecules. This makes it a suitable candidate for biosensor applications. The glasslike nature and good optical quality allows for light addressable entities to be incorporated and accessed using spectroscopy. This type of matrix, once formed, can be anything from an ordered gel to a robust glassy block depending on the aging process. In this work we apply confocal microscopy and time-resolved fluorescence techniques to study both rotational and lateral diffusion with aging time within a silica sol−gel derived monolith. An enzyme, horseradish peroxidase, was labeled with Alexa Fluor 488 and rotation related to both the enzyme and the probe monitored during the matrix aging process. Diffusion coefficients of between ca. 0.5×10^{-7} and 4×10^{-7} cm^2 s^{-1} were obtained from preliminary FRAP measurements of fluorescein and correlated to differences in the catalytic activity of HRP incorporated in the monolith.

Introduction

Matrices derived from the sol−gel technique have proved to be good hosts for a variety of substances. These range from laser dyes and porphyrins, used to study optical effects, to biologically active molecules.[1] Depending on stage of development (or on how far the matrix forming reaction has progressed) the host can be anything from a viscous solution or ordered gel to, finally, a robust glassy structure of good optical quality with a highly porous nature.[2,3] This coupled with the ability to allow access to external liquids and gases make these matrices highly suitable for use as optically addressable sensors (when doped with the appropriate sensing entity). The low processing temperature makes the sol−gel-derived matrix a suitable host for biological species, such as peptides, proteins, including enzymes, and to form biosensors.[4,5] The use of enzymes in sol−gel-derived media, for example, provides a form of immobilization (important for reuse, cost, and environmental factors) while allowing accessibility for the enzyme to function as a biocatalyst. This action can be followed using spectroscopic means by either making use of intrinsic protein fluorescence or using extrinsic probes. The latter are advantageous as they can be chosen for their selectivity. Previous work has shown that encapsulation within a sol−gel-derived medium can restrict protein mobility,[6] although sol−gel media are also known to template around the encapsulated protein.[4] It is therefore important to gain an understanding of guest−host interactions. Time-resolved fluorescence anisotropy[7] and fluorescence recovery after photobleaching (FRAP)[8,9] are appropriate techniques with which to obtain information concerning the mobility of the encapsulated bio-molecule. FRAP probes the translational diffusion, whereas time-resolved fluorescence anisotropy measurements reveals information about rotational diffusion. The separation of translational and rotational diffusion has yielded insight into protein association in viscous media,[10] and in particular the combination of FRAP and time-resolved fluorescence anisotropy measurements have previously been employed, for example, in the study of the rheological properties of cell cytoplasm using green fluorescent protein.[11] However, to our knowledge, FRAP has been scantily applied to the study of sol−gel-derived media.

In this work we elucidate information concerning the diffusion within the sol−gel-derived media, which are important in their use for biosensor purposes, by studying the enzyme horseradish peroxidase, which was covalently labeled with Alexa Fluor 488 (AF) before sol−gel encapsulation. This involved taking time-resolved fluorescence lifetime and anisotropy[12] measurements during the aging process to monitor the enzymes mobility. Confocal microscopy[13,14] was used to ascertain a homogeneous distribution of the labeled enzyme and, making use of FRAP, the diffusion of fluorescein (Fs) incorporated within the matrix was monitored and correlated with the observed catalytic activity of the encapsulated enzyme.

Materials and Methods

Sol−Gel Preparation. Sol−gel-derived media were produced in the form of a monolith using a standard 10 mm path length plastic cuvette for a mould. The sol was produced by mixing 9 mL of tetraethyl orthosilicate (Aldrich) with 3 mL of water containing 0.2 mL of 0.01 M HCl. This mixture was placed in an ultrasonic bath for 1 h before being placed in a freezer (−18 °C) for about a month. The matrices were formed by taking 2 mL of the sol and mixing it with 2 mL of pH 7 phosphate buffer solution containing the labeled enzyme. Gelling occurred within minutes, and the gels were stored in a refrigerator (at 4 °C).

* To whom correspondence should be addressed. E-mail: graham@fisica.uminho.pt. Phone: 00351-253604320. Fax: 00351-253678981.

10.1021/jp066021i CCC: $37.00
Published on Web 03/13/2007

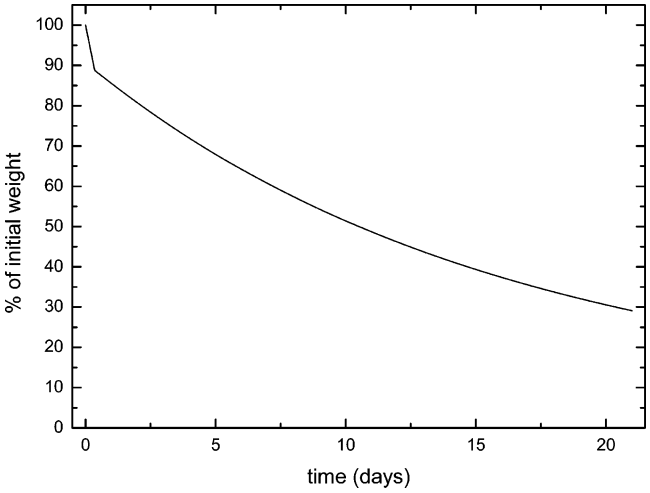

Figure 1. Depiction of the percentage change in weight of a sol−gel-derived matrix with time when kept at 4 °C.

After approximately 12 h it was possible to remove the monoliths from their moulds, and they were rinsed with distilled water. The resultant monoliths at the time of their first measurement were approximately $9 \times 9 \times 30$ mm^3 in size. After a month this was down to ca. $^1/_8$ of the initial volume. The resultant loss of weight with time as the matrix hardens and solvent is expelled is depicted in Figure 1.

Enzyme Labeling. Horseradish peroxidase [HRP, EC 1.11.1.7] from Sigma, which has a molecular weight about 44 000,[15] was labeled and then purified following the provided protocol using a Molecular Probes Alexa Fluor 488 protein labeling kit (A-10235) from Invitrogen S. A. The molecular weight of Alexa Fluor 488 is ~885, which is low in comparison to the enzyme.

Enzyme Activity. The relative horseradish activity was obtained from the oxidation of ABTS (2,2′-azino-bis(3-ethylbenzothiazoline-6-sulfonic acid) diammonium salt, from Sigma) by hydrogen peroxide (H_2O_2, 37% Aldrich). The formation of the oxidized ABTS radical, as seen by an increase in the band at 414 nm in the absorption spectrum, was monitored.[16] Slices from sol−gel monoliths (ca. 100 mg in weight) were placed in a cuvette containing 3 mL of $\sim 2.5 \times 10^{-5}$ M ABTS and 4 μL of H_2O_2 in buffer solution. This gave a ratio of approximately 1:10 for ABTS:H_2O_2. The absorption spectrum over a range 250−500 nm was recorded; both before the addition of the enzyme containing monolith slice and after the kinetic study was complete. The kinetic study commenced on the addition of the matrix and measurements were performed at room temperature.

Measurements. Spectra were recorded using a Shimadzu UV-3101PC (absorption) and a SPEX Fluorolog (fluorescence) spectrophotometer. Time-resolved measurements used a single-photon counting apparatus equipped with a NanoLED-01 excitation source (HORIBA, Jobin Yvon, IBH Ltd. Glasgow, Scotland). The fluorescence emission was wavelength selected using filters (550 nm cutoff unless stated otherwise) and detected with a Hamamatsu R2949 photomultiplier. Data analysis was performed with IBH DAS6 software and the goodness of fit judged in terms of a χ^2 value and weighted residuals. The fluorescence decays were analyzed by using a sum of exponentials, employing a nonlinear least-squares reconvolution analysis of the form

$$I(t) = \sum_{i=1}^{n} \alpha_i \exp(-t/\tau_i) \tag{1}$$

where $I(t)$ is the fluorescence intensity I at time t as measured in photon counts, α_i are the pre-exponential factors (which are given normalized to unity), and τ is the fluorescence lifetime and n the number of exponentials.

After reconvolution a nominal time resolution of ca. 150 ps was attained. Errors are given as three standard deviations throughout.

Time-resolved fluorescence anisotropy decays (eq 2) of Alexa Fluor labeled HRP were analyzed making use of the impulse response function and values for the rotational correlation time τ_R plus the initial r_0 and limiting anisotropies r_∞ were recovered

$$r(t) = (r_0 - r_\infty) \exp(-t/\tau_R) + r_\infty \tag{2}$$

In the case of a hindered rotation ($r_\infty \neq 0$) the "wobble in cone" model[17] was employed and the cone angle θ calculated using eq 3[7]

$$2\left(\frac{r_\infty}{r_0}\right)^{1/2} = \cos^2\theta + \cos\theta \tag{3}$$

This has been applied in polymer systems.[18] The rotational correlation time is related to the viscosity η of the system through the Stokes−Einstein relation

$$\tau_R = \frac{V\eta}{kT} \tag{4}$$

where k is the Boltzmann constant, T the absolute temperature, and V the effective volume, theoretical calculations of which were obtained from the qualitative structure activity relationships (QSAR) computation using Hyperchem 7 software on geometrically optimized molecular structures (using a PM3 model for the dyes or AMBER for HRP).[19]

FRAP of fluorescein (MW 332) in the sol−gel medium was performed using an inverted confocal microscope (Leica TCS SP2) with a ×63 water immersion objective and 488 nm excitation from an argon ion laser. To obtain FRAP measurements, five initial intensity images were taken over an area of 288^2 μm^2, at 2 s intervals. The laser power was then increased and an area of approximately 100^2 μm^2 was photobleached. The fluorescence recovery of this area was monitored by reducing the laser power and recording images every 5 s for 200 s (512 × 512 pixels, 400 Hz line scan rate). The recovery curves obtained were then corrected for photobleaching during recovery by selecting a sample region away from the bleached region of interest and thus obtaining a fluorescence intensity vs time curve (control curve) and dividing the raw recovery curve by it. The corrected recovery of intensity with time (assuming bleaching above and below the focal plane) was fitted to a curve of the form (eq 5)[20] using Origin software

$$I(t) = A(1 - \exp(-kt)) + C \tag{5}$$

where I is the fluorescence intensity and k is a time constant. A is the final plateau intensity after the recovery minus the initial intensity after bleaching ($F_\infty - F_0$), and C is the initial intensity after bleaching F_0. The time taken to return to half of the final intensity $t_{1/2} = (\ln 2)/k$ and is related to the translational diffusion coefficient D by

$$D = 0.88\omega^2/4t_{1/2} \tag{6}$$

where ω is the radius of the bleached area (ca. 50 μm).[9,20,21]

Time-resolved fluorescence anisotropy measurements of Alexa Fluor 488 encapsulated in the sol−gel matrix were also

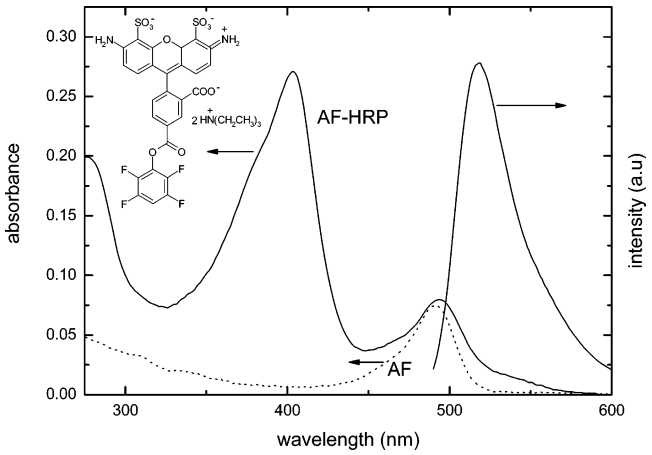

Figure 2. Absorption and emission spectra of AF-HRP, along with the absorption spectrum of uncoupled AF (dotted line) for comparison. Inset is the structure of AF.

TABLE 1: Absorption and Fluorescence Data for Unbound AF and AF Bound to HRP in Buffer Solution

measurement		AF	AF-HRP
steady state	absorption max (nm)	491	494
	fluorescence max (nm)	516	518
lifetime	τ_1 (ns)	4.04 ± 0.01	4.11 ± 0.03
	τ_2 (ns)		2.03 ± 0.15
	α_1	1	0.84
	α_2		0.16
	χ^2	1.08	1.05
anisotropy	τ_{r1} (ns)	0.25 ± 0.09	0.51 ± 0.21
	τ_{r2} (ns)		7.87 ± 2.40
	α_1	1	0.63
	α_2		0.37
	r_0	0.260	0.285
	r_∞	0	0.009
	θ		74°
	χ^2	1.02	1.01

performed with a Becker & Hickl SPC 830 card in a 3GHz, Pentium IV, 1GB RAM computer running Windows XP. A 467-nm pulsed diode laser (PLP-10 470, Hamamatsu, optical pulse width 90 ps) was employed to excite the fluorescein in the sol−gels at a repetition rate of 20 MHz. The fluorescence was detected through a 525 ± 25 nm interference filter using a cooled PMC100-01 detector (Becker & Hickl, based on a Hamamatsu H5772P-01 photomultiplier).

Results and Discussion

Dye−Enzyme Interaction. After the coupling reaction and purification, fractions containing the dye−enzyme conjugate (AF-HRP) and the uncoupled dye (AF) were obtained. Both steady state and time-resolved measurements were performed for both AF-HRP and AF in solution prior to incorporation into the sol−gel-derived media. The spectra of the conjugate are shown in Figure 2. On coupling, a slight red shift is observed in both the absorption and fluorescence spectra of AF, as shown in Table 1. The time-resolved data showed a more discernible change going from a monoexponential decay to a biexponential decay for the AF-HRP conjugate. Here the difference was the emergence of a small contribution of a shorter-lived component. The origin of this component requires investigation but may relate to the covalent linkage and/or the local amino acid residues. Another difference was noted in the time-resolved anisotropy data. For uncoupled AF, as expected, a very fast rotational time, close to the resolution of our equipment, was observed. This is similar to that calculated using eq 4, with V calculated from the QSAR properties for AF (assuming a viscosity of 0.89 cP and temperature of 300 K), which returned 0.30 ns. The anisotropy decay obtained for the AF-HRP conjugate required two rotational correlation times to provide an acceptable fit. The shorter one we attribute to the dye rotation, while the longer one reflects the motion of the whole of the enzyme. A similar trend has been previously reported.[22] Our calculation of this rotational time returned a close value of 6.5ns. As the r_∞ value does not go to zero, this implies a small degree of hindrance (cone angle of 74° according to eq 3), which is not surprising as the AF is covalently bound to the enzyme.

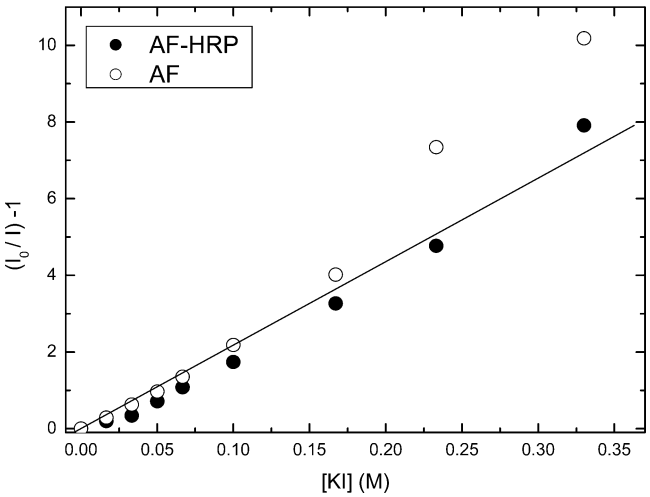

Figure 3. Change in steady-state fluorescence intensities (I) of AF and AF-HRP in solution on addition of KI. The line depicts a simple fit to the Stern−Volmer equation for the AF-HRP data.

As the hindrance is small, it is indicative that AF most likely binds to the exterior of the HRP. To verify this, a quenching study using potassium iodide (KI) was performed. The effect of the quencher on the steady-state fluorescence is shown in Figure 3. The plot shows that at lower quencher concentrations there is little difference between the unbound and bound AF. A Stern−Volmer quenching constant of 21.7 M^{-1} was obtained from the slope of the line[23] represented in the figure. At higher concentrations of KI there is an upward trend in the data, which may signify the presence of other processes other than a straightforward dynamic quenching mechanism. This is not surprising considering the charged nature of the quencher. However, the similarity of the curves at low quencher concentration is supportive of the probe attached to the exterior of the enzyme.

Rotational Diffusion. Time-resolved anisotropy measurements were performed on the AF-HRP conjugate following its addition into the matrix forming reaction mixture. The sample gelled within minutes and measurements were carried out over a period of time, in which the sample changed from a solid gel to a glassy robust matrix, occupying about an $^1/_8$ of the volume of the initial gel. The encapsulated enzyme is retained within the pore structure[24] and confocal microscopy showed the distribution within the matrix to be uniform. Time-resolved fluorescence anisotropy measurements were made to provide a means by which to monitor the enzymes rotational mobility. Figure 4 illustrates the change in rotational correlation time with aging time. This shows that on incorporation there is an initial increase in the rotational correlation time, probably because of a raised viscosity as the matrix gels, after which the value returns close to that of the conjugate in solution, as the pore structure starts to form. These data indicate that, although the matrix network is contracting, the local environment of the enzyme is

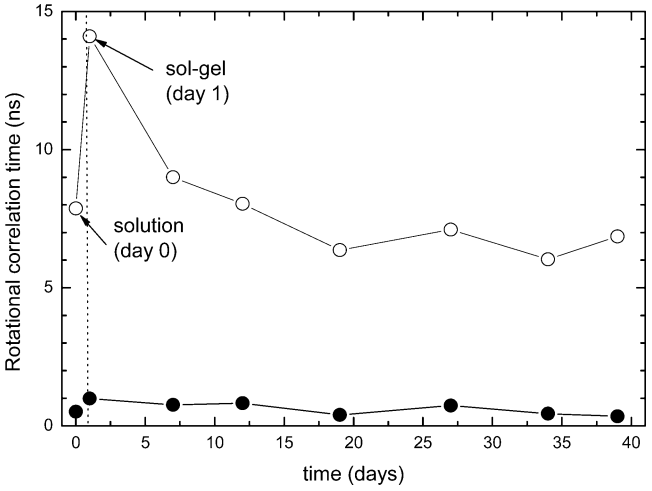

Figure 4. Rotational correlation times for AF bound to HRP, both before and after incorporation into a sol−gel-derived monolith. The open symbols we relate to the rotation of the entire enzyme, while the closed symbols are ascribed to the probes own rotation.

TABLE 2: Recovery Rates, k (s^{-1}), and Times, $\tau_{1/2}$ (s), Obtained Using Eq 5 for the Intensity of Fs Fluorescence from the FRAP Measurements with Matrix Aging Time

time (days)	k (s^{-1})	$\tau_{1/2}$ (s)
2	0.048 ± 0.012	14 ± 4
6	0.015 ± 0.002	45 ± 6
8	0.0143 ± 0.0005	49 ± 2
10	0.0067 ± 0.0005	100 ± 7
13	0.0057 ± 0.0006	121 ± 13
15	0.0052 ± 0.0006	132 ± 30
20	0.0036 ± 0.0003	191 ± 17
27	0.0041 ± 0.0004	169 ± 14
35	0.0040 ± 0.0005	174 ± 20

comparatively stable, unlike that encountered in another study.[6] It should be noted that a slight decrease in the cone angle was observed, dropping to ca. 53° after 7 days and dropping by another few degrees over the remaining period. This may indicate slight changes in the enzyme conformation, in agreement with previous studies with this system.[24] Over the same time period the fluorescence lifetime data exhibited little variation from the corresponding data in solution, thus reinforcing the suitability of this system.

Translational Diffusion. Although the enzyme appears free to rotate within the pore structure of the matrix, it is important to ascertain if it is free to relocate within the matrix and, if it is to be catalytically active, accessible to its substrate. In order to verify this, preliminary FRAP measurements using a confocal microscope were performed with fluorescein (Fs) incorporated in the same type of sol−gel-derived monolith. FRAP has previously been used to characterize sol−gel-produced matrices, where dyes were found to diffuse only if the matrices were hydrated.[25] The results from the FRAP measurements are given in Table 2. From these measurements the diffusion with aging time was calculated and is depicted in Figure 5. The trend seen is reminiscent of the rotational correlation time (Figure 4), in that there is a decrease with time. However, in terms of diffusion, this is the inverse of what is seen from the rotational information, as shown in Figure 6. An explanation for this is that the rotational diffusion provides information concerning the pore environment, while the translation diffusion is giving information relating to interconnections between pores, since the network shrinks with time (see Figure 1) and this hinders free translational diffusion. Thus, the two measurement sets are complementary in following changes in matrix morphology. We,

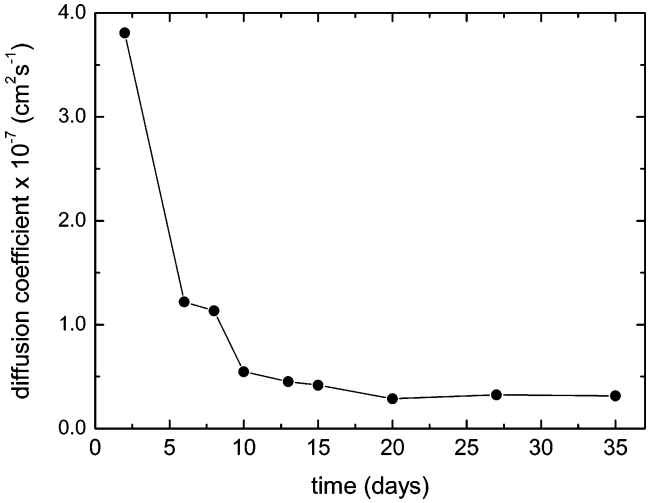

Figure 5. Diffusion coefficient for Fs in a sol−gel-derived monolith with aging time, calculated from the data in Table 2, according to eq 6.

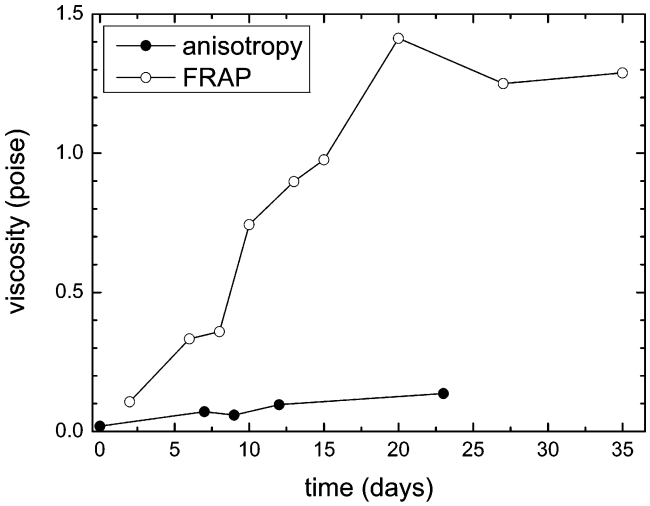

Figure 6. Comparison of the sensed viscosity obtained using FRAP measurements of Fs and anisotropy measurements of unbound AF. Measurements were performed using confocal microscopy.

of course, are looking at the average behavior of many Fs molecules. Work at the single molecule level has elucidated that pore size is influential on the diffusion within sol−gel-derived monoliths and that two different components relating to mobility can be seen.[26,27] In comparison with that work, the diffusion coefficients we find are several orders of magnitude greater than those found for a silica gel with pores ca. 22 nm in diameter and using a larger probe molecule. The rotational diffusion of our enzyme hints that there is no significant interaction with the pore, thus the pores inhabited by the enzyme should be significantly larger than the dimension of the enzyme.[18] Most probably the HRP efficiently templates the pore size of its host. It should also be noted that the diffusion coefficient that we recover has contributions of pore entrapment and the viscosity of the interpore connections, with the main contribution ascribed to the latter.

Host Viscosity. As both anisotropy and FRAP appear complementary a comparison of the viscosity sensed by the dye molecule was made using the anisotropy of unbound AF and the FRAP measurements of Fs. The outcome is given in Figure 6. With aging time a difference is clearly seen between the two forms of measurement and correlates with the formation and stabilization of the pore structure, while the wide interconnec-

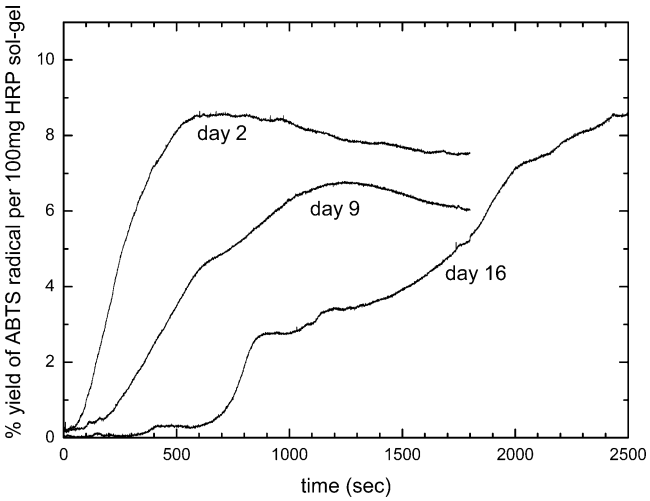

Figure 7. Catalytic activity of HRP in a sol−gel-derived monolith as a function of time. Monitored by observing the ABTS radical formation at 414 nm.

tions between the pores constrict with time thus causing an enhancement of the effective viscosity. It appears from our data, performed using silica monoliths, that the pores probed by the dyes still retain solvent, unlike a previous confocal study, where the pores were dry[25] but in agreement with previous work that we have performed.[28]

Effect of Aging Time on Catalytic Activity. A clear objective of the incorporation of enzymes for biosensor applications is that, as well as being encapsulated, the enzyme exhibits catalytic activity and is accessible to its substrate. With this goal in mind, catalytic activity measurements using hydrogen peroxide and ABTS were performed during the aging period by cutting a slice from the monolith and monitoring the evolution of the ABTS radical.[16] The resultant kinetic traces are shown in Figure 7. These show that the enzyme exhibits catalytic activity, albeit at a lower level than in solution, as we have previously reported.[24] The main feature of these kinetic traces is that the maximum level of activity attained is similar, the major differences relate to the time that it takes to reach this level. As the rotational diffusion data show that the enzyme environment is more or less stable, this increase in time is ascribed to a narrowing of the pore interconnection, with its associated increase in viscosity. It should also be noted that a narrowing of the pore interconnections can also lead to a reduction in observed catalytic activity, as repulsion exists between the negatively charged ABST and the silica matrix through which it must diffuse.[16]

Conclusion

In the silica sol−gel-derived matrices we have observed that encapsulated HRP is able to exhibit rotational diffusion; however, translational diffusion becomes limited with matrix aging time. This affects the rate at which the enzyme is able to display catalytic activity, as it takes longer for the substrate to diffuse through the host matrix. The use of FRAP and time-resolved fluorescence anisotropy techniques were found to be complementary in probing changes in matrix morphology and its effect on encapsulated enzymes, which are necessary in their usage for biosensor applications.

Acknowledgment. We would like to thank Eric Reits and John Presley for their helpful hints regarding the FRAP analysis. Financial support through the "Treaty of Windsor" (CRUP-British Council No. B-37/06) is also acknowledged.

References and Notes

(1) Reisfeld, R. *J. Non-Cryst. Solids* **1990**, *121*, 254.
(2) Brinker, C. J.; Scherer, G. W. *Sol-Gel Science: The Physics and Chemistry of Sol-Gel Processing*; Academic Press: 1990.
(3) Hungerford, G.; Pereira, M. R.; Ferreira, J. A.; Viseu, T. M. R.; Coelho, A. F.; Ferreira, M. I. C.; Suhling, K. *J. Fluorescence* **2002**, *12*, 397.
(4) Jin, W.; Brennan, J. D. *Anal. Chim. Acta* **2002**, *461*, 1.
(5) Pierre, A. C. *Biocatalysis Biotransformations* **2004**, *22*, 145.
(6) Gottfried, D. S.; Kagan, A.; Hoffman, B. M.; Friedman, J. M. *J. Phys. Chem. B* **1999**, *103*, 2803.
(7) Steiner, R. In *Topics in fluorescence spectroscopy*; Lakowicz, J. R., Ed.; Plenum Press: New York, 1991; Vol. 2, pp 1−52.
(8) Braeckmans, K.; Peeters, L.; Sanders, N. N.; De Smedt, S. C.; Demeester, J. *Biophys. J.* **2003**, *85*, 2240.
(9) Reits, E. A. J.; Neefjes, J. J. *Nature Cell Biol.* **2001**, *3*, E145.
(10) Kuttner, Y. Y.; Kozer, N.; Segal, E.; Schreiber, G.; Haran, G. *J. Am. Chem. Soc.* **2005**, *127*, 15138.
(11) Swaminathan, R.; Hoang, C. P.; Verkman, A. S. *Biophys. J.* **1997**, *72*, 1900.
(12) Suhling, K.; Siegel, J.; Lanigan, P. M. P.; Lévêque-Fort, S.; Webb, S. E. D.; Phillips, D.; Davis, D. M.; French, P. M. W. *Opt. Lett.* **2004**, *29*, 584.
(13) Suhling, K.; French, P. M. W.; Phillips, D. *Photochem. Photobiol. Sci.* **2005**, *4*, 13.
(14) Suhling, K. In *Methods Express, Cell Imaging*; Stephens, D., Ed.; Scion Publishing: Bloxham, 2006; pp 219−245.
(15) Welinder, K. G. *Eur. J. Biochem.* **1979**, *96*, 483.
(16) Kadnikova, E. N.; Kostić, N. M. *J. Mol. Catal. B* **2002**, *18*, 39.
(17) Kinoshita, K.; Kawato, S.; Ikeyami, A. *Biophys. J.* **1977**, *20*, 289.
(18) Egelhaaf, H.-J.; Lehr, B.; Hof, M.; Häfner, A.; Fritz, H.; Schneider, F. W.; Bayer, E.; Oelkrug, D. *J. Fluorescence* **2000**, *10*, 383.
(19) Hungerford, G.; Rei, A.; Ferreira, M. I. C. *FEBS J.* **2005**, *272*, 6161.
(20) Presley, J. F. In *Methods Express, Cell Imaging*; Stephens, D., Ed.; Scion Publishing Ltd: Bloxham, 2006; pp 119−142.
(21) Axelrod, D.; Koppel, D. E.; Schlessinger, J.; Elson, E.; Webb, W. W. *Biophys. J.* **1976**, *16*, 1055.
(22) Alexiev, U.; Rimke, I.; Pöhlmann, T. *J. Mol. Biol.* **2003**, *328*, 705.
(23) Eftink, M. R. In *Topics in fluorescence spectroscopy*; Lakowicz, J. R., Ed.; Plenum Press: New York, 1991; Vol. 2, pp 53−126.
(24) Hungerford, G.; Rei, A.; Ferreira, M. I. C. *Biophys. Chem.* **2006**, *120*, 81.
(25) Weiss, A. M.; Saraidarov, T.; Reisfeld, R. *Opt. Mat.* **2001**, *16*, 15.
(26) Hellriegel, C.; Kirstein, J.; Bräuchle, C.; Latour, V.; Pigot, T.; Olivier, R.; Lacombe, S.; Brown, R.; Guieu, V.; Payrastre, C.; Izquierdo, A.; Mocho, P. *J. Phys. Chem. B* **2004**, *108*, 14699.
(27) Hellriegel, C.; Kirstein, J.; Bräuchle, C. *New J. Phys.* **2005**, *7*, 23.
(28) Hungerford, G.; Suhling, K.; Ferreira, J. A. *J. Photochem. Photobiol. A* **1999**, *129*, 71.